

# Results

The results of the analyses described above take one of two forms: direct inspection of posterior parameter estimates, and downstream estimates of diversity and diversification rates based on posterior predictive simulations.

## Posterior parameter estimates

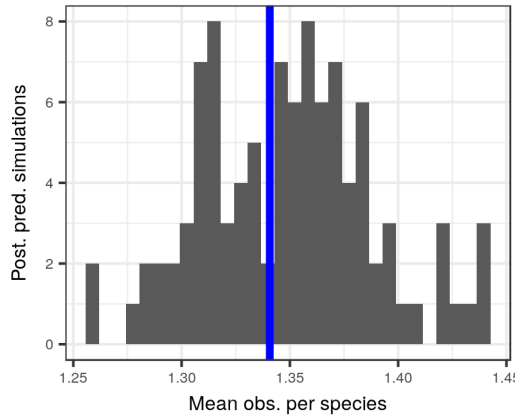


Figure 1: Comparison of the average observed number of occurrences per species (blue line) to the average number of occurrences from 100 posterior predictive datasets using the posterior estimates from the pure-presence and birth-death models.

## Analysis of diversity

All of the analyses of diversification and macroevolutionary rates has been done using only the birth-death model because of the model's better posterior predictive check performance (Fig. 1).

The general pattern of the estimated North American total mammal diversity for the Cenozoic is “stable” in that diversity fluctuates around a constant mean standing diversity, does not fluctuate wildly and rapidly over the Cenozoic, and demonstrates no sustained directional trends (Fig. 15a). In

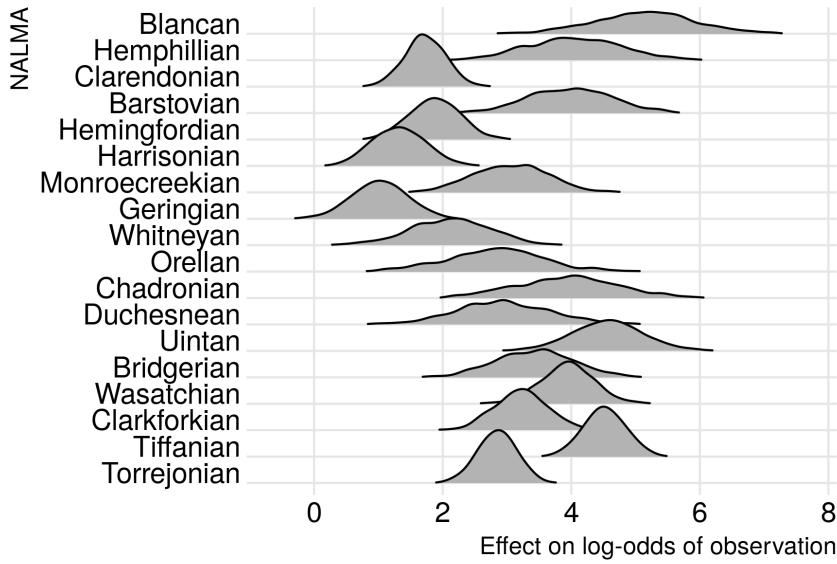


Figure 2

broad strokes, the first 15 or so million years of the Cenozoic are characterized by first an increase and then a decline in standing diversity at approximately 45-50 Mya (early-middle Eocene). Following this decline, standing diversity is broadly constant from 45 to 18 Mya (early Miocene). After this, there is a rapid spike in diversity followed by a slight decline in diversity up to the Recent.

The pattern exhibited by the diversity history estimated in this study (Fig. 15a) has some major similarities with previous mammal diversity curves [?]: both curves begin with an increase in diversity most of the major increases in diversity are retained including the large diversity spike during the Miocene. Unlike subsampling based approaches to estimating diversity [?], I'm able to interpolate over unsampled/poorly sampled time periods because of how the hierarchical model can share information across the different units [?]; for cases like unsampled temporal bins, this may lead to estimates with high uncertainty, but that is preferable to no estimate at all. Finally, the Bayesian framework here gives a distribution of possible estimates of diversity allowing for direct inspection of the uncertainty of our inferences, something that is preferable to both traditional and resampling based confidence interval estimates [?]. Note that my time series of estimated diversity begins at a

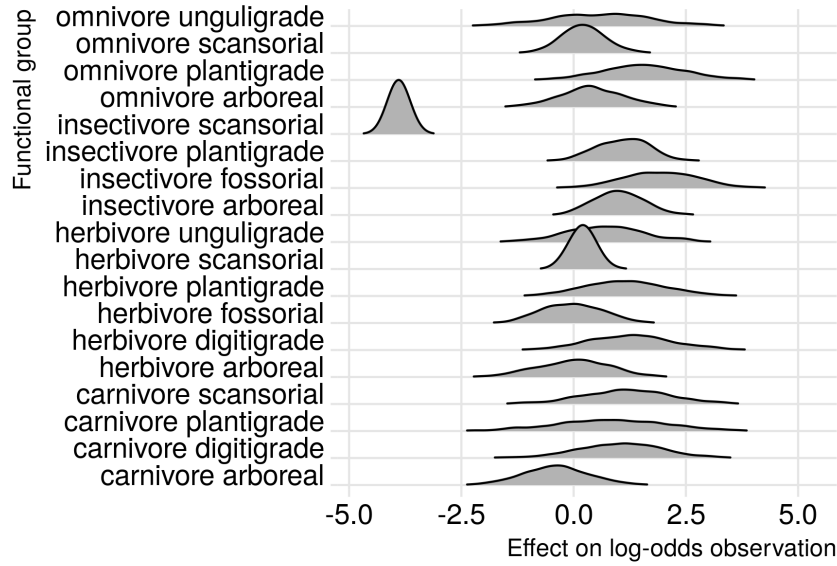


Figure 3

slightly different point than that of ? ] and that the time intervals used by ? ] are slightly shorter than those used here, so this may cause some of the minor differences between the curves. Also, please note that the diversity values are plotted at the “ceiling” of each temporal interval and not at the midpoint (Fig. 15a).

When viewed through the lens of diversification rate, some of the structure behind the estimated diversity history begins to take shape (Fig. 15b). For most of the Cenozoic, the diversification rate hovers around zero, punctuated by both positive and negative spikes. The largest spike in diversification rate is at 16 Mya, which is early Oligocene (Fig. 15b). Other notable increases in diversification rate occur 56, 46, 22, 18, and 6 Mya (Table 5), though the last of these may be due to edge effects surrounding the partial-identifiability of  $p_{t=T}$ . Notable decreases in diversification rate occur at 54, 50, 48, 44, 40, 34, 30, 24, 20, 16, 12, and 8 Mya (Table 5), meaning that diversification rate has more major decreases than increases. While diversification rates significantly lower than average are more common than diversification rates greater than average, when diversification rate does increase it is with a greater magnitude than most decreases (Fig. 15b). Given that diversification rate more closely resembles origination rate than extinction rate (Fig. 15b, ??,

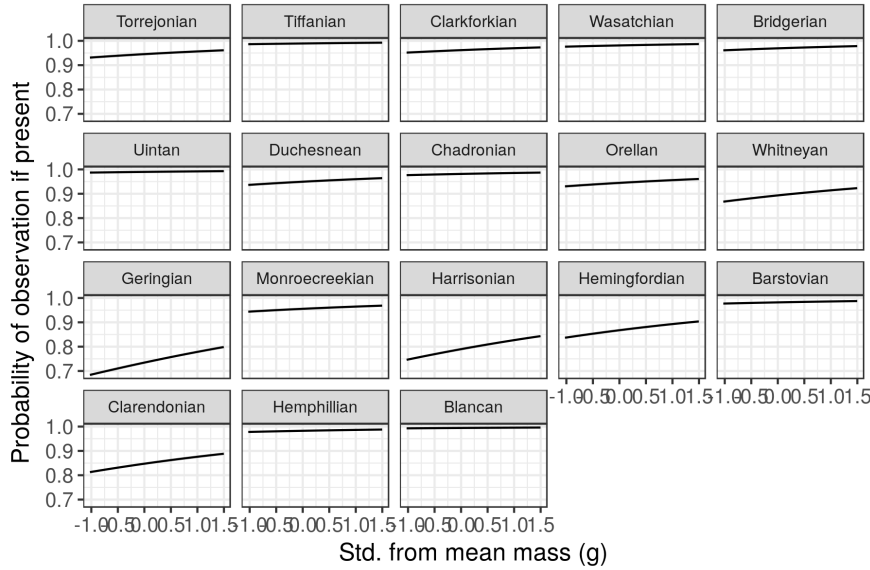


Figure 4: Estimates of the effect of species mass on probability of sampling a present species ( $p$ ). Mass has been log-transformed, centered, and rescaled; this means that a mass of 0 corresponds to the mean of log-mass of all observed species and that mass is in standard deviation units. Estimates are from both the pure-presence and birth-death models.

??), these decreases in diversification rate may be indicative of “depletions” (failure to replace extinct taxa) rather than pulses of extinction.

The estimates from this study of per capita origination and extinction rates for the entire species pool (Fig. ??, ??) are very different from the origination and extinction rates estimated by ? ]. The two most striking difference are the very different estimates of extinction rate between the two studies and the very different scales of the origination rate estimates. This may be due to the fundamentally different way these rates are calculated, and how the diversification process was modeled. The per capita rates estimated in this study follow straight from the definition of a per capita rate (e.g. number of originations between time  $t$  and  $t + 1$  divided by the diversity at time  $t$ ) while the rates calculated in ? ] are based on log ratios of standing diversity.

The comparison between per capita origination and extinction rate estimates reveals how diversification rate is formed (Fig. ??, ??). As expected given

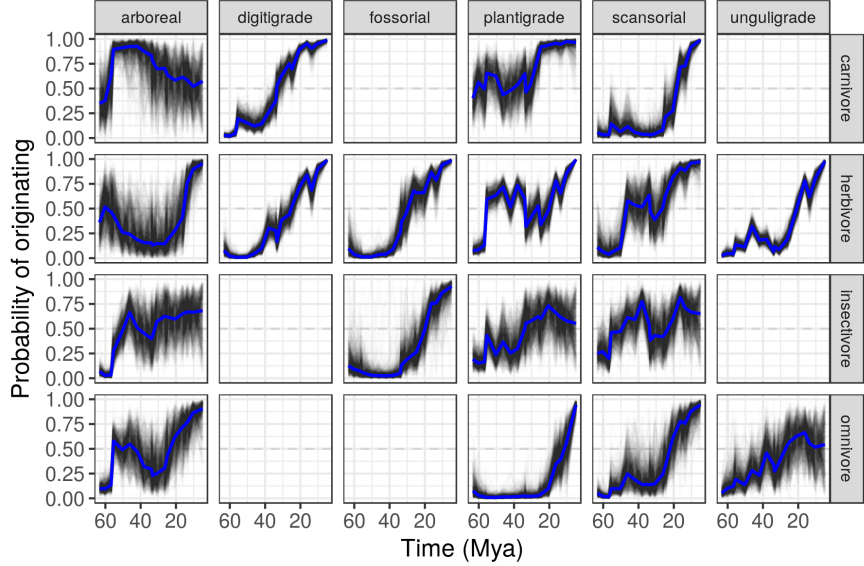


Figure 5: Probability of a mammal ecotype origination probabilities at each time point as estimated from the birth-death model. Each panel depicts 100 random samples from the model’s posterior. The columns are by locomotor category and rows by dietary category; their intersections are the observed and analyzed ecotypes. Panels with no lines are ecotypes not observed in the dataset.

previous inspection of the ecotype specific estimates of origination and survival probabilities from the birth-death model, diversification rate seems most driven by changes in origination rate as opposed to extinction rate. Extinction rate, on the other hand, demonstrates an almost saw-toothed pattern around a constant mean (Fig. ??). These results are broadly consistent with those from previous analyses of North American mammals diversity and diversification [? ? ? ].

Diversity partitioned by ecotype reveals a lot of the complexity behind the pattern of mammal diversity for the Cenozoic (Fig. 16).

Arboreal ecotypes obtain peak diversity early in the Cenozoic and then decline for the rest of the time series, becoming increasingly rare or absent as diversity approaches the Recent (Fig. 16). Arboreal herbivores and omnivores obtain peak diversity at the beginning of the Cenozoic then go into decline

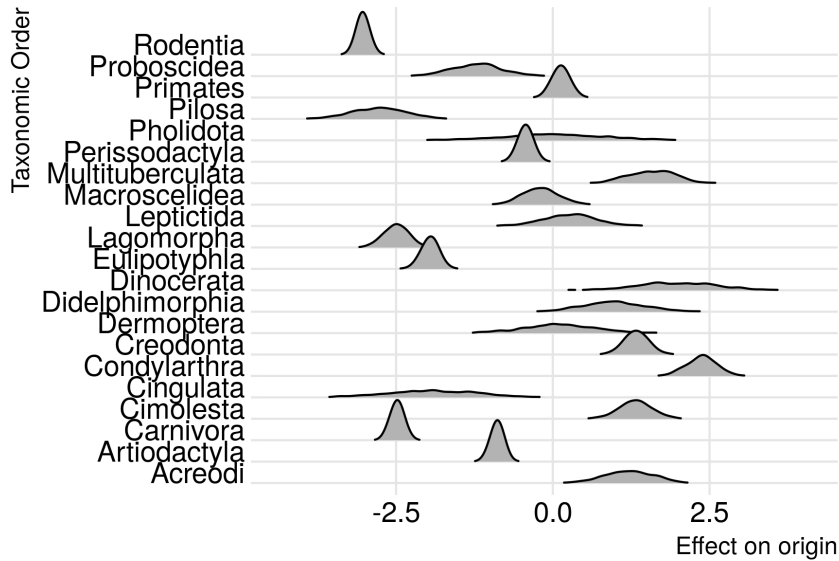


Figure 6

while remaining a small part of the species pool, while arboreal carnivores and insectivores obtain peak diversity 52-50 Mya and then quickly decline and become extremely rare or entirely absent from the species pool. This is consistent with increasing extinction risk in the Neogene compared to the Paleogene as proposed by [? ].

The diversity of digitigrade and unguligrade herbivores increases over the Cenozoic (Fig. 16). In contrast, plantigrade herbivore diversity does not have a single, broad-strokes pattern; instead, diversity increases, decreases, and may have then increased till the Recent. In contrast, fossorial and scansorial herbivores demonstrate a much flatter history of diversity, with a slight increase in diversity that over time is more pronounced among fossorial taxa than scansorial taxa. The expansion of digitigrade and unguligrade herbivores over the Cenozoic is consistent with the gradual expansion of grasslands which these ecotypes are better adapted to than closed environments [? ? ].

Digitigrade carnivores have a multi-modal diversity history, with peaks at 54-52 and 12-10 Mya (Fig.16). Between these two peaks digitigrade carnivore diversity dips below average diversity following the first peak and then grows slowly until the second peak. Plantigrade carnivores obtain peak diversity

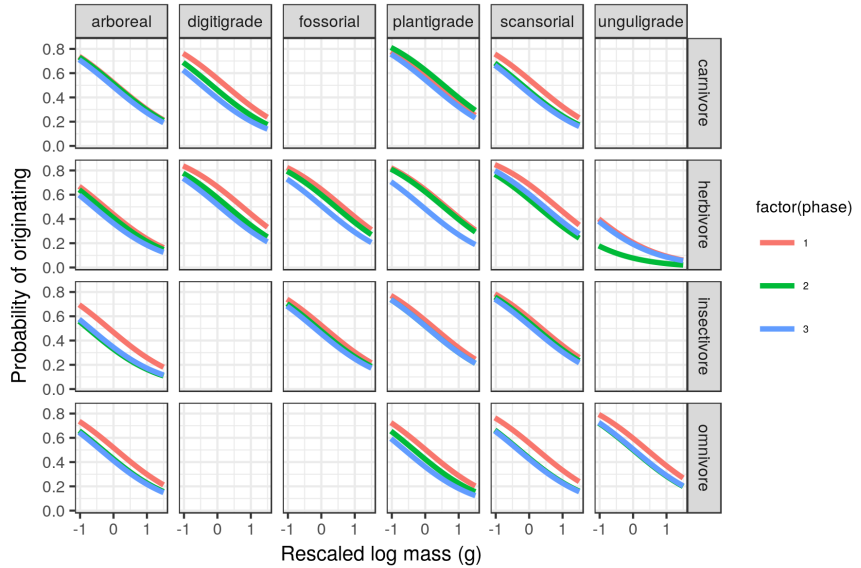


Figure 7: Mean estimate of the effect of species mass on the probability of a species originating for each of the three plant phases. The effect of mass is considered constant over time and that the only aspect of the model that changes with plant phase is the intercept of the relationship between mass and origination. The three plant phases are indicated by the color of the line. Mass has been log-transformed, centered, and rescaled; this means that a mass of 0 corresponds to the mean of log-mass of all observed species and that mass is in standard deviation units. For clarity, only the mean estimates of the effects of mass and plant phase are plotted.

in the early Cenozoic and then maintain a relatively stable diversity until another peak at the end of the Cenozoic. The generally flat diversity history digitigrade carnivores lacks any sustained temporal trends and seems to reflect previous findings of limited diversity in spite of constant turnover and morphological evolution [? ? ?]

There are some broad similarities in diversity histories of insectivorous and omnivorous taxa. The diversity histories of arboreal, plantigrade, and scansorial insectivorous taxa all demonstrate a decreasing pattern with time, while fossorial insectivores have a flat diversity history with a peak approximately 10 Mya (Fig. 16). Arboreal and scansorial omnivores decrease in diversity from their initial peaks early in the Cenozoic, and plantigrade omnivores

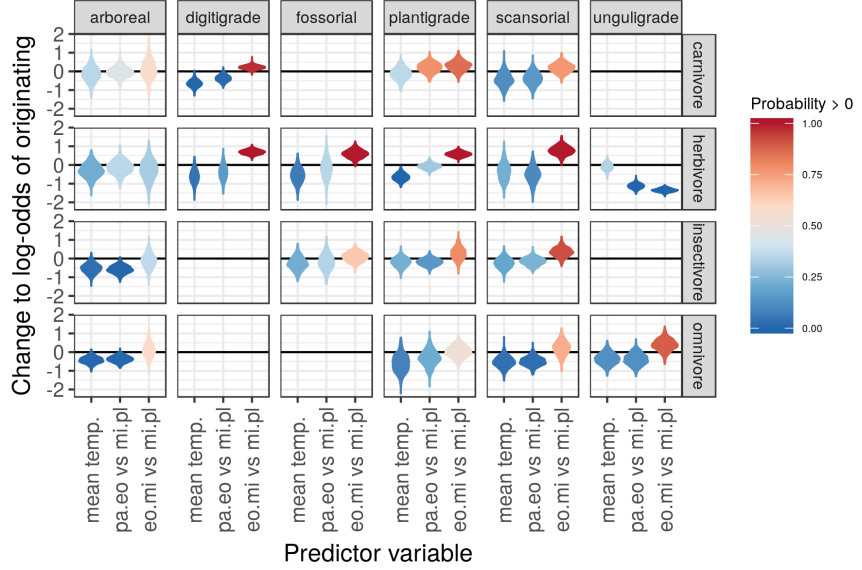


Figure 8: Estimated effects of the group-level covariates describing environmental context on log-odds of species origination. These estimates are from the birth-death model. What is plotted is a violin of the distribution of 1000 samples from the approximate posterior. The effect of plant phase graphed here is calculated as Phase 1=  $\gamma_{phase\ 1}$ , Phase 2=  $\gamma_{phase\ 1} + \gamma_{phase\ 2}$ , and so on.

have a generally flat diversity history with a sudden peak in diversity late in the Cenozoic (Fig. 16). Unguligrade omnivores also demonstrate a possible decrease in diversity over the Cenozoic, but not as clearly as arboreal and scansorial omnivores.

The waxing and waning of the mammal ecotypes is obvious when comparing changes to estimated relative log-mean of diversity (Fig. 17). While ecotype diversity does appear to change gradually, there are definite changes to the relative contributions of the ecotypes to the regional species pool. All arboreal ecotypes clearly decrease in relative diversity over the Cenozoic. In contrast the digitigrade herbivore, fossorial herbivore, scansorial herbivore, and unculigrade herbivore ecotypes which increase in relative diversity over the Cenozoic. The digitigrade carnivore ecotype increases in relative diversity until approximately the start of the Neogene, after which it maintains a generally constant relative diversity; this is consistent with previous observations of

Table 1: Posterior probability of the differences in the log-odds of an ecotype originating based on plant phase.

	P(Eo.Mi > 0)	P(Pa.Eo > 0)	P(Eo.Mi > Pa.Eo)
arboreal carnivore	0.575	0.447	0.598
digitigrade carnivore	0.976	0.017	0.998
plantigrade carnivore	0.857	0.780	0.578
scansorial carnivore	0.768	0.154	0.889
arboreal herbivore	0.318	0.357	0.428
digitigrade herbivore	1.000	0.161	0.995
fossilorial herbivore	0.999	0.353	0.926
plantigrade herbivore	1.000	0.304	0.998
scansorial herbivore	0.999	0.108	0.998
unguligrade herbivore	0.000	0.000	0.100
arboreal insectivore	0.364	0.003	0.857
fossilorial insectivore	0.645	0.341	0.708
plantigrade insectivore	0.794	0.148	0.881
scansorial insectivore	0.916	0.235	0.940
arboreal omnivore	0.590	0.006	0.882
plantigrade omnivore	0.524	0.209	0.762
scansorial omnivore	0.713	0.027	0.938
unguligrade omnivore	0.888	0.127	0.960

constant or density-dependent diversity of the canid guild for the Neogene [? ? ], a guild that overlaps with the digitigrade carnivore ecotype. Plantigrade herbivores remain a constant relative contribution to ecotypic diversity. These results support the hypothesis of a gradual transition from the early Paleogene with a region with more available habitat for arboreal taxa and less available habitat for many digitigrade and unguligrade taxa, to an environment where arboreal taxa are absent from the species pool and digitigrade and unguligrade taxa are much more dominant (Fig. 17). It is the relative contributions of digitigrade carnivores, digitigrade herbivores, and unguligrade herbivores which really shape the regional species pool of the Neogene.

Many of the estimated ecotype-specific diversity histories share a similar increase in diversity in the late Cenozoic, 16-14 Mya (Fig. 16). These increases are either sustained or temporary and are seen in digitigrade carnivores, plantigrade carnivores, scansorial carnivores, unguligrade herbivores, fossilorial

Table 2: Posterior probability that the effects of the two temperature covariates on the log-odds of an ecotype origination are greater than 0. What is estimated is the probability that these estimates are greater than 0; high or low probabilities indicate the “strength” of the covariate in that direction (positive and negative, respectively). These estimates are from the birth-death model.

	$P(\gamma_{temp\ mean} > 0)$
arboreal carnivore	0.355
digitigrade carnivore	0.001
plantigrade carnivore	0.358
scansorial carnivore	0.121
arboreal herbivore	0.219
digitigrade herbivore	0.045
fossorial herbivore	0.067
plantigrade herbivore	0.000
scansorial herbivore	0.221
unguligrade herbivore	0.339
arboreal insectivore	0.027
fossorial insectivore	0.219
plantigrade insectivore	0.224
scansorial insectivore	0.192
arboreal omnivore	0.009
plantigrade omnivore	0.087
scansorial omnivore	0.035
unguligrade omnivore	0.129

insectivores, and plantigrade omnivores.

Table 3: Posterior probability of the differences in the log-odds of an ecotype surviving based on plant phase.

	P(Eo.Mi > 0)	P(Pa.Eo > 0)	P(Eo.Mi > Pa.Eo)
arboreal carnivore	0.297	0.560	0.328
digitigrade carnivore	0.786	0.367	0.743
plantigrade carnivore	0.411	0.744	0.273
scansorial carnivore	0.428	0.445	0.486
arboreal herbivore	0.256	0.768	0.174
digitigrade herbivore	1.000	0.400	0.942
fossorial herbivore	0.696	0.563	0.565
plantigrade herbivore	0.659	0.508	0.596
scansorial herbivore	0.616	0.539	0.531
unguligrade herbivore	0.000	0.102	0.012
arboreal insectivore	0.289	0.483	0.368
fossorial insectivore	0.532	0.420	0.592
plantigrade insectivore	0.499	0.361	0.605
scansorial insectivore	0.443	0.252	0.634
arboreal omnivore	0.651	0.597	0.591
plantigrade omnivore	0.417	0.549	0.393
scansorial omnivore	0.486	0.525	0.487
unguligrade omnivore	0.929	0.521	0.844

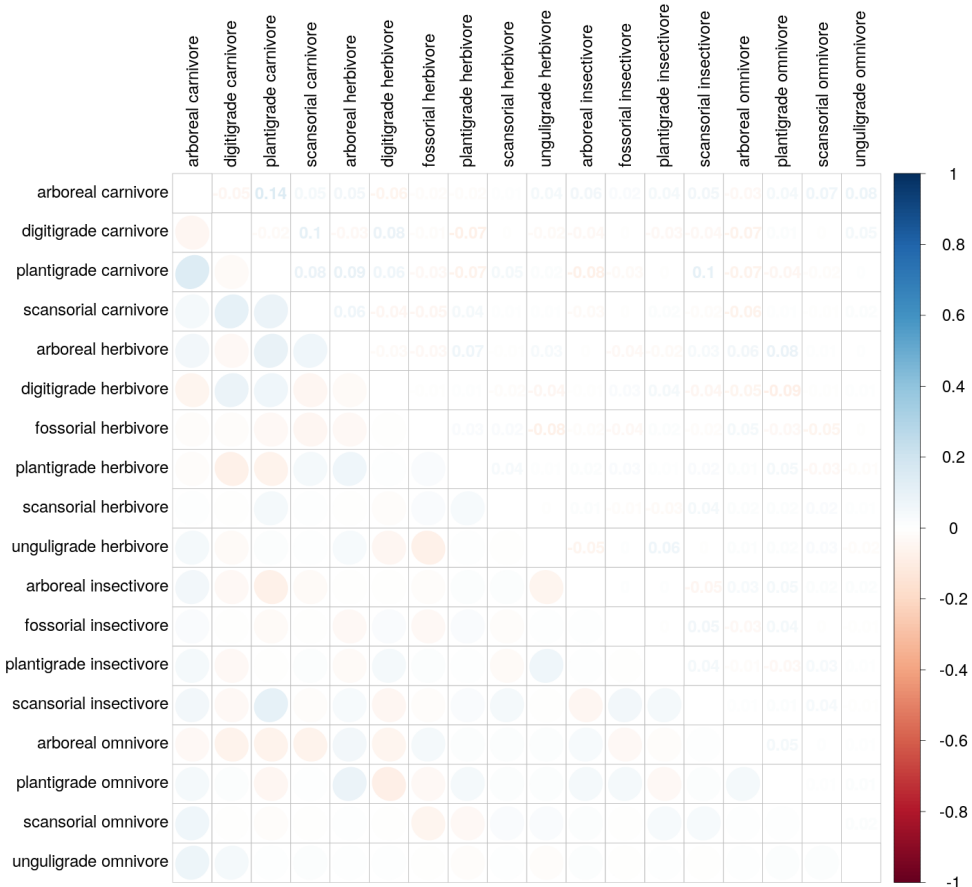


Figure 9: Posterior mean estimates of the correlations in origination probability between the mammal ecotypes. The lower triangle of the matrix is populated with ellipses corresponding to the level of correlation between the two ecotypes, while the upper triangle of the matrix corresponds to the mean estimated correlation between ecotypes. Darker values correspond to a greater magnitude of correlation with blue values corresponding to a positive correlation and red values a negative correlation.

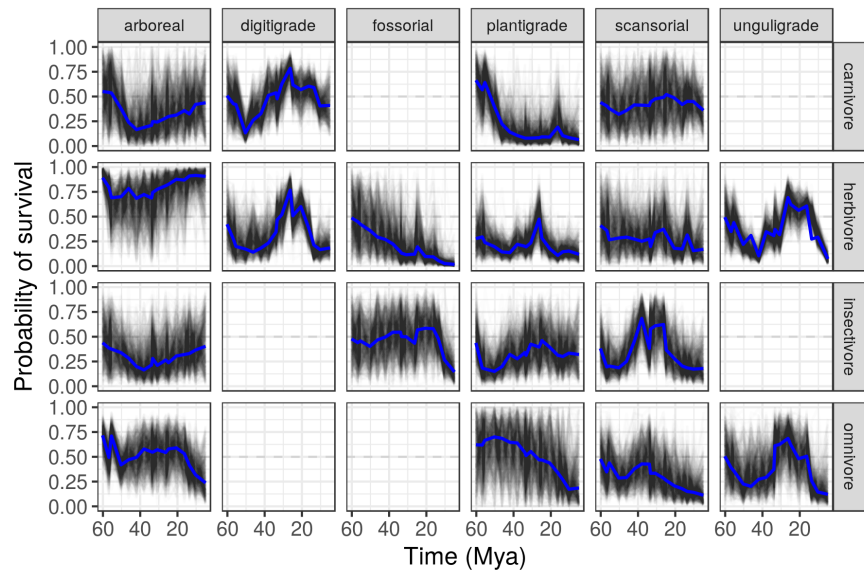


Figure 10: Probability of a mammal ecotype survival probabilities at each time point as estimated from the birth-death model. Each panel depicts 100 random samples from the model's posterior. The columns are by locomotor category and rows by dietary category; their intersections are the observed and analyzed ecotypes. Panels with no lines are ecotypes not observed in the dataset.

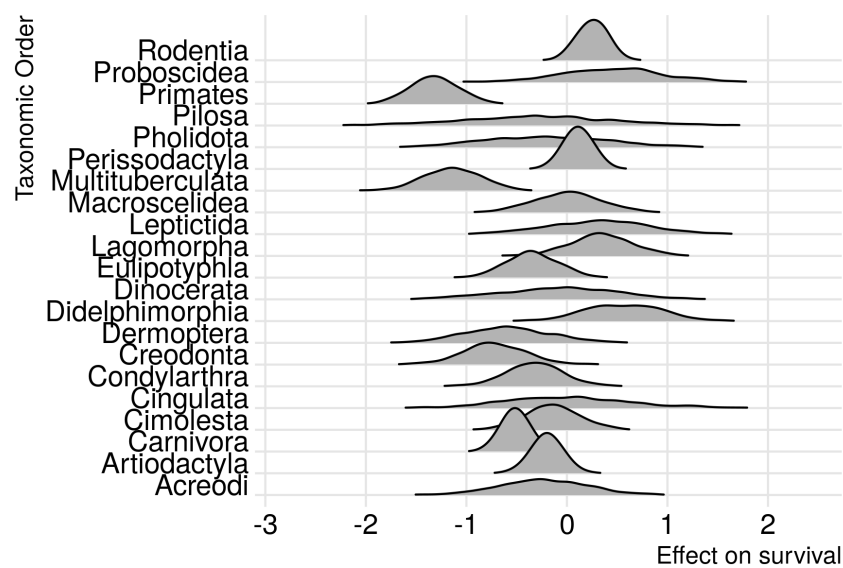


Figure 11

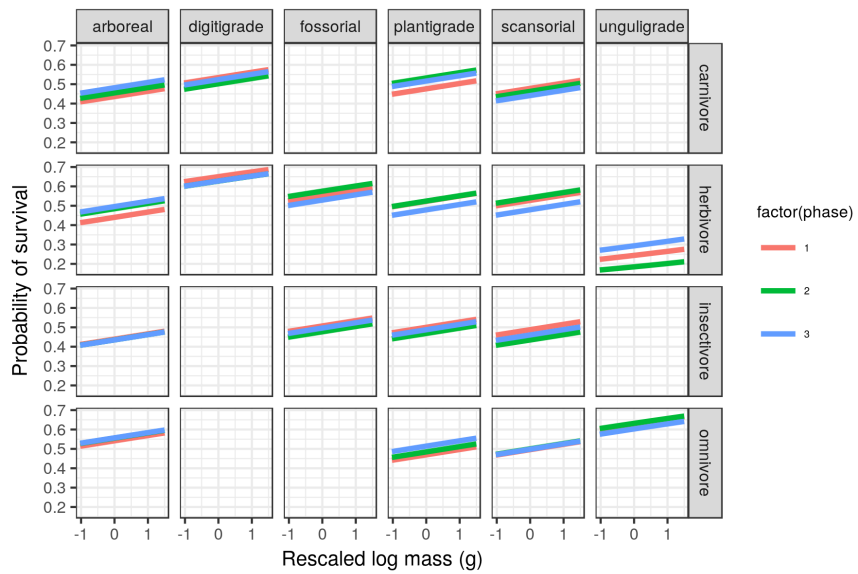


Figure 12: Mean estimate of the effect of species mass on the probability of a species survival for each of the three plant phases. The effect of mass is considered constant over time and that the only aspect of the model that changes with plant phase is the intercept of the relationship between mass and survival. The three plant phases are indicated by the color of the line. Mass has been log-transformed, centered, and rescaled; this means that a mass of 0 corresponds to the mean of log-mass of all observed species and that mass is in standard deviation units. For clarity, only the mean estimates of the effects of mass and plant plant are plotted.

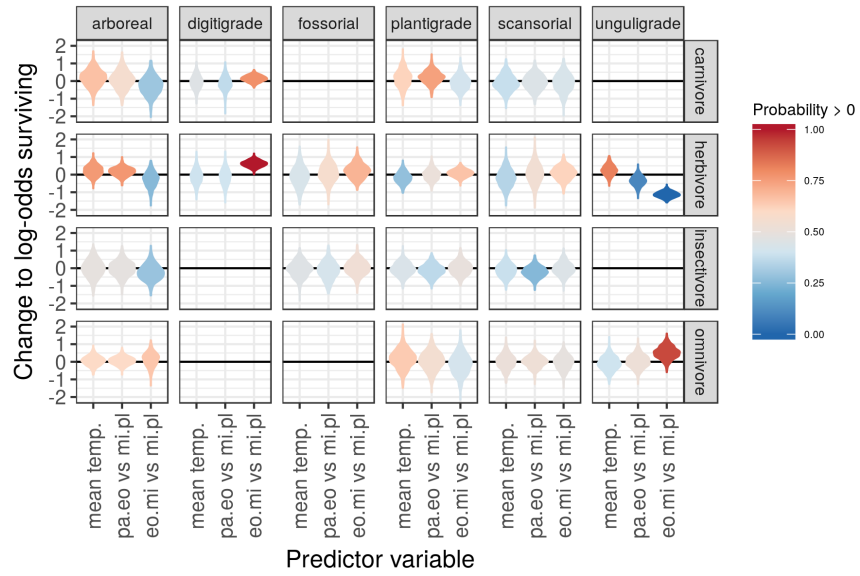


Figure 13: Estimated effects of the group-level covariates describing environmental context on log-odds of species survival. These estimates are from the birth-death model. What is plotted is a violin of the distribution of 1000 samples from the approximate posterior. The effect of plant phase graphed here is calculated as Phase 1=  $\gamma_{phase\ 1}$ , Phase 2=  $\gamma_{phase\ 1} + \gamma_{phase\ 2}$ , and so on.

Table 4: Posterior probability that the effects of the two temperature covariates on the log-odds of an ecotype survival are greater than 0. What is estimated is the probability that these estimates are greater than 0; high or low probabilities indicate the “strength” of the covariate in that direction (positive and negative, respectively). These estimates are from the birth-death model.

	$P(\gamma_{temp\ mean} > 0)$
arboreal carnivore	0.665
digitigrade carnivore	0.453
plantigrade carnivore	0.618
scansorial carnivore	0.380
arboreal herbivore	0.761
digitigrade herbivore	0.395
fossorial herbivore	0.429
plantigrade herbivore	0.279
scansorial herbivore	0.345
unguligrade herbivore	0.818
arboreal insectivore	0.489
fossorial insectivore	0.452
plantigrade insectivore	0.435
scansorial insectivore	0.384
arboreal omnivore	0.600
plantigrade omnivore	0.639
scansorial omnivore	0.512
unguligrade omnivore	0.396

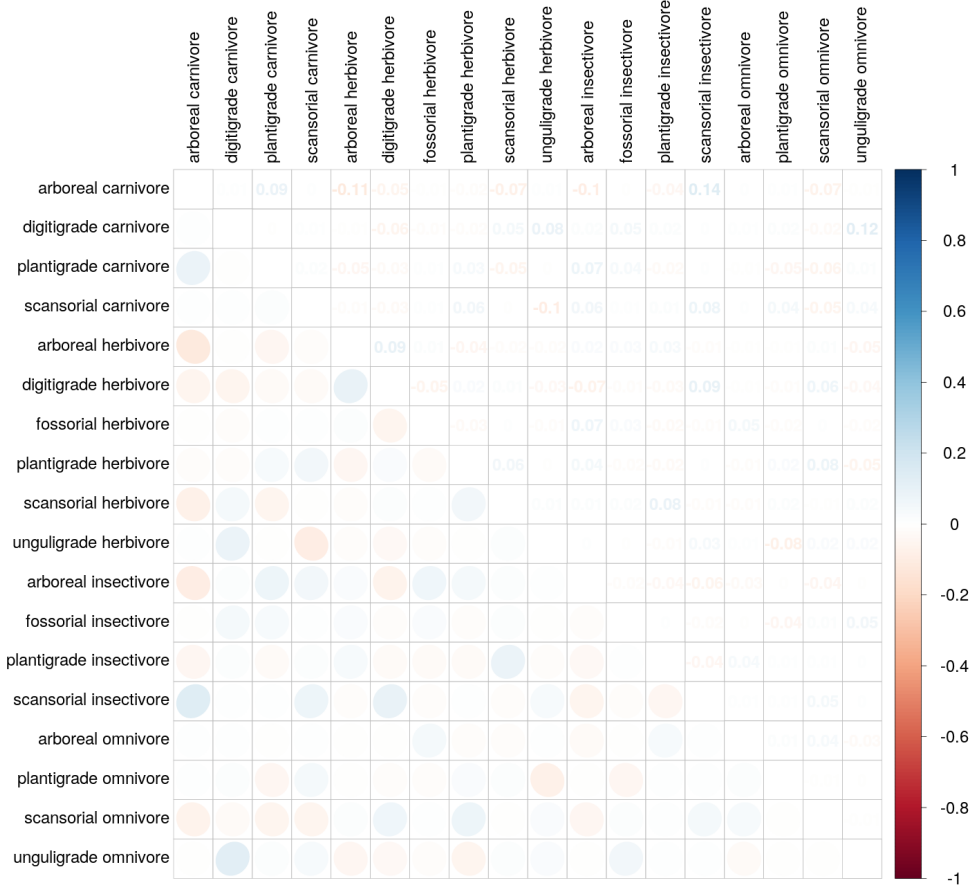


Figure 14: Posterior mean estimates of the correlations in survival probability between the mammal ecotypes. The lower triangle of the matrix is populated with ellipses corresponding to the level of correlation between the two ecotypes, while the upper triangle of the matrix corresponds to the mean estimated correlation between ecotypes. Darker values correspond to a greater magnitude of correlation with blue values corresponding to a positive correlation and red values a negative correlation.

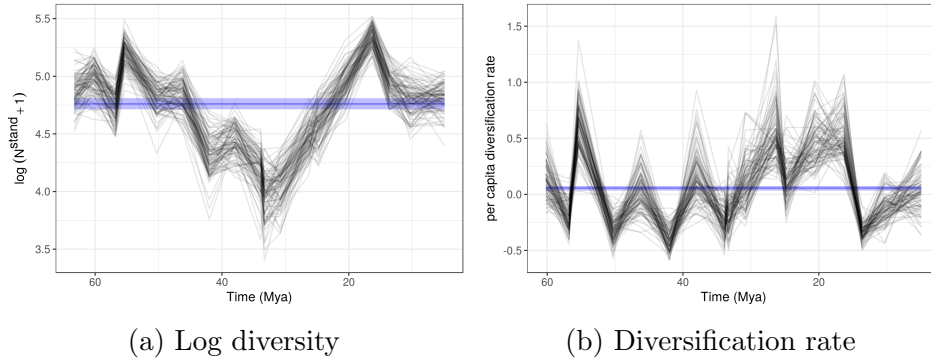


Figure 15: Posterior estimates of the time series of Cenozoic North American mammal diversity and its characteristic macroevolutionary rates; all estimates are from the birth-death model and 100 posterior draws are plotted to indicate the uncertainty in these estimates. The blue horizontal strip corresponds to the 80% credible interval of estimated mean standing diversity, diversification rate, origination rate, and extinction rate respectively; the median estimate is also indicated. What is also plotted is the The dramatic differences between diversity estimates at the first and second time points and the penultimate and last time points in this series are caused by well known edge effects in discrete-time birth-death models caused by  $p_{-,t=1}$  and  $p_{-,t=T}$  being partially unidentifiable [?]; the hierarchical modeling strategy used here helps mitigate these effects but they are still present [? ?]. Diversification rate is in units of species gained per species present per time unit (2 My), origination rate is in units of species originating per species present per time unit, and extinction rate is in units of species becoming extinct per species present per time unit.

Table 5: Posterior probabilities of diversity  $N_t^{stand}$  or diversification rate  $D_t^{rate}$  being greater than average standing diversity  $\bar{N}^{stand}$  or average diversification rate  $\bar{D}^{rate}$  for the whole Cenozoic. The “Time” column corresponds to the top of each of the temporal bins. Diversification rate can not be estimated for the last time point because it is unknown how many more species originated or went extinct following this temporal bin. The estimates are from the birth-death model.

NALMA	$P(N_t^{stand} > \bar{N}^{stand})$	$P(D_t^{rate} > \bar{D}^{rate})$
Torrejonian	0.79	
Tiffanian	0.95	0.67
Clarkforkian	0.50	0.03
Wasatchian	1.00	0.99
Bridgerian	0.69	0.00
Uintan	0.75	0.45
Duchesnean	0.00	0.00
Chadronian	0.01	0.70
Orellan	0.00	0.01
Whitneyan	0.00	0.09
Geringian	0.00	0.57
Monroecreekian	0.01	1.00
Harrisonian	0.11	0.67
Hemingfordian	0.96	0.99
Barstovian	1.00	1.00
Clarendonian	0.93	0.00
Hemphillian	0.63	0.10
Blancan	0.73	0.43

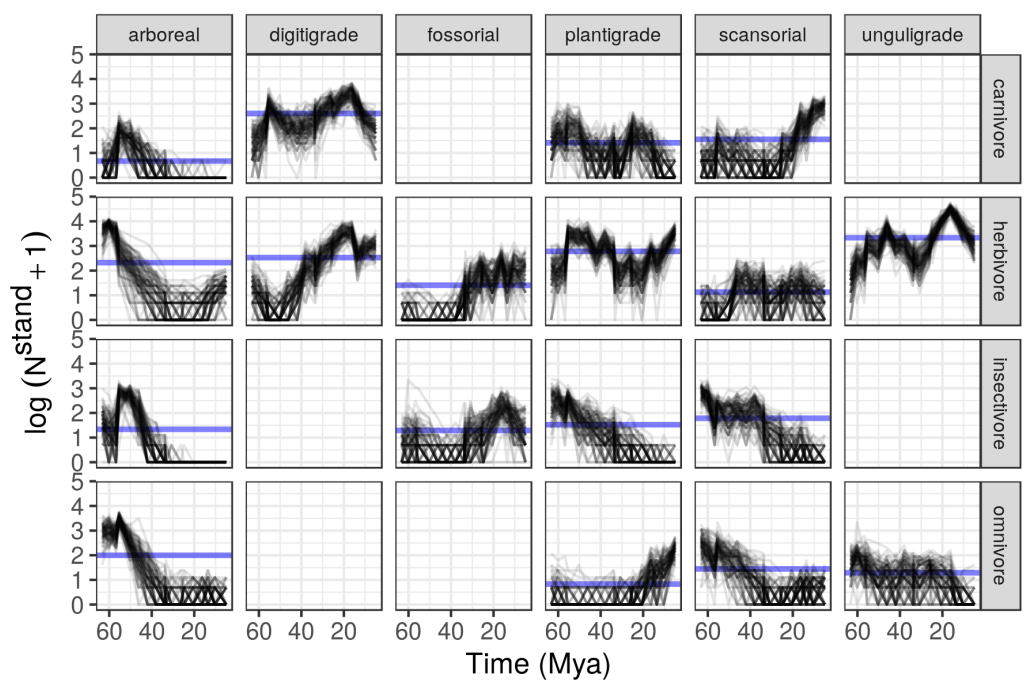


Figure 16: Posterior of standing log-diversity of North American mammals by ecotype for the Cenozoic as estimated from the birth-death model; 100 posterior draws are plotted to indicate the uncertainty in these estimates and what is technically plotted is log of diversity plus 1.

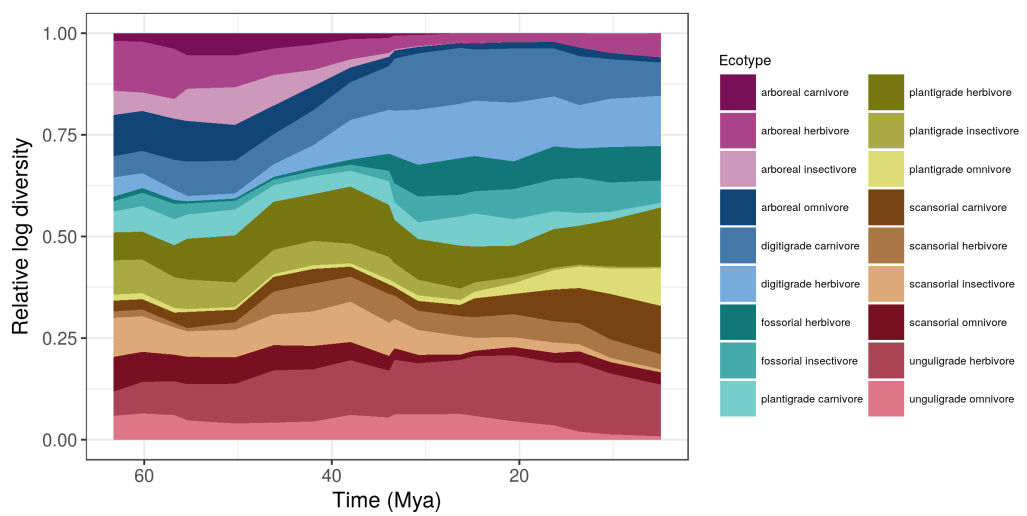


Figure 17: Mean posterior estimate of relative log standing diversity of 18 North American mammal ecotypes for the Cenozoic. These estimates are calculated from 100 posterior estimates of the true occurrence matrix  $z$  as estimated from the birth-death model.